

Performance Comparison of Gyrocardiogram and Seismocardiogram Signals in Valvular Heart Disease Assessment

Ecem Erin¹ and Beren Semiz²

¹Department of Physics, Bogazici University, Istanbul, Turkey

²Department of Electrical and Electronics Engineering, Koc University, Istanbul, Turkey

Keywords: Valvular Heart Disease, Seismocardiogram, Gyrocardiogram, Cardiovascular Health Monitoring, Biomedical Signal Processing.


Abstract: Cardiovascular diseases have been identified as one of the leading causes of mortality worldwide. Among these diseases, valvular heart diseases (VHDs) have a greater impact on the population. The existing methods for VHD assessment are expensive and only applicable within clinical environments. Hence, there is a need for accessible and cost-efficient systems to provide continuous VHD monitoring. As stenosis and regurgitation are characterized by the change in the blood flow patterns, it was hypothesized that angular acceleration (gyrocardiogram, GCG) could capture the differences in blood flow and changes in cardiovascular parameters better than linear acceleration (seismocardiogram, SCG). In this work, a publicly available dataset including 36 patients with stenosis and 44 patients with regurgitation was used. The SCG and GCG signals were first divided into 10-second long segments. From each segment, five features were extracted from all axes and used to train the SCG- and GCG-based XGBoost models. Overall, the GCG-based model resulted in better performance in distinguishing between the stenosis and regurgitation cases: the precision, recall and accuracy values were 94.7, 94.5, and 94.5 for the SCG, and 96.0, 95.9 and 95.9 for the GCG, respectively. Predictive performances of SCG and GCG models on the cardiovascular parameters were also investigated and resulted in (SCG, GCG) mean absolute percent errors of (19.4, 20.6), (15.5, 14.5), (12.0, 13.1) for ejection fraction, left ventricular end diastolic dimension and left ventricle posterior wall thickness, respectively. These results showed that in addition to SCG, GCG could also be used for VHD evaluation and potentially be employed in continuous monitoring systems.

1 INTRODUCTION

According to the 2020 report by the World Health Organization (WHO), cardiovascular diseases have been identified as one of the leading causes of mortality worldwide (WHO, 2020). Among cardiovascular diseases, valvular heart diseases (VHDs) have a greater impact on the population and result in higher mortality rates (Go et al., 2013). In the heart, four main heart valves are present: tricuspid valve, aortic valve, mitral valve, and pulmonary valve (Klabunde, 2011; Svensson, 2008). VHDs primarily emerge due to the impairments in these valves. These impairments can be group under two main categories: stenosis and regurgitation, which can affect any of the aforementioned valves. In the case of stenosis, the valve opening narrows, leading to inadequate blood outflow. On the other hand, regurgitation refers to the valve's fail-

ure to prevent the backward flow of blood (Svensson, 2008).

While echocardiography, magnetic resonance imaging, cardiac catheterization, and computed tomography can be used to monitor VHDs, these methods are costly and only available in clinical settings (Svensson, 2008). Hence, there is a need for accessible and cost-efficient systems to provide non-invasive and continuous VHD monitoring. Recent advancements in wearable sensor research have paved the way to collect physiological signals from the body non-invasively. As these signals directly originate from the underlying anatomy, they can provide valuable information regarding the current physiological status of the subject. Among these physiological signals, seismocardiogram (SCG) has been widely leveraged in wearable system design. SCG originates from the contraction of the heart and corresponds to the resulting micro chest vibrations (Inan et al., 2014). Mostly,

 <https://orcid.org/0000-0002-7544-5974>

tri-axial accelerometers are used to collect the SCG signal in three directions: lateral, head-to-foot and dorso-ventral. On the other hand, recent studies have shown that utilizing gyroscope-based vibrations could offer enhanced capabilities in detecting heart activity and blood movement compared to accelerometers (Yang et al., 2017; Yang and Tavassolian, 2017; Jafari Tadi et al., 2017; Shandhi et al., 2019). However, the performance of gyrocardiogram (GCG) in VHD assessment is still an open research question.

From physics perspective, accelerometers measure linear acceleration; whereas gyroscope can capture dynamic angular velocity in three axes (yaw, pitch, and roll) (Faisal et al., 2019). Considering that the stenosis and regurgitation impairments exhibit different blood flow characteristics, it was hypothesized that GCG could capture the differences in blood flow and changes in cardiovascular parameters better than SCG. The contributions of this study can thus be listed as follows: for the first time to the best of our knowledge, (i) the performance of GCG in VHD assessment was studied and compared with the SCG performance, (ii) contributions of the spectral features and individual SCG and GCG axes (X, Y, and Z) in VHD assessment were investigated, (iii) predictive performances of SCG and GCG models on the cardiovascular parameters (ejection fraction, left ventricular end diastolic dimension and left ventricle posterior wall thickness) under stenosis and regurgitation conditions were investigated.

2 METHODS

2.1 Dataset Description

In this study, *An Open-Access Database for the Evaluation of Cardio-Mechanical Signals From Patients With Valvular Heart Disease*, which includes seismocardiogram (SCG), gyrocardiogram (GCG) and electrocardiogram (ECG) signals, was used (Yang et al., 2021). The participants were identified as having different forms of valvular heart diseases (VHD), including mitral valve stenosis (MS), aortic stenosis (AS), aortic valve regurgitation (AR), mitral valve regurgitation (MR), and tricuspid valve regurgitation (TR). Each specific VHD was indicated by a label whether if the disease is present.

The SCG, ECG and GCG signals were collected using commercially available Shimmer system (Shimmer 3 ECG module, Shimmer Sensing, United Kingdom) while the subject was in supine position. For the analysis, only the tri-axial SCG and GCG signals were used. The X, Y, and Z directions of the SCG

and GCG signals were representing the vibrations in the lateral, head-to-foot, and dorso-ventral directions, respectively.

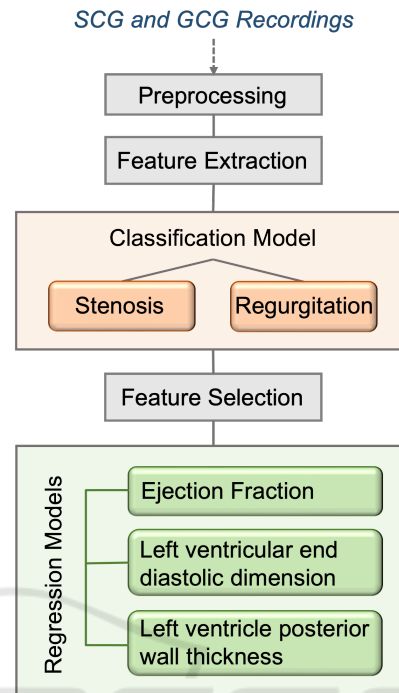


Figure 1: Study Overview.

2.2 Pre-Processing and Data Preparation

As the goal was to investigate the performance of SCG and GCG in stenosis and regurgitation assessment, two different sub-datasets were generated: one having only SCG signals, the other one including only the GCG signals. In both sub-datasets, there were 36 patients with stenosis and 44 patients with regurgitation present either of the valves. It should be noted that these signals were simultaneously acquired from the same subjects and the classification and regression tasks were employed on the same samples. Thus the data was comparable. However, some GCG signals were shorter in duration.

In the datasets, some recordings had a sampling rate of 256 Hz while the others had a rate of 512 Hz. To ensure standardization, all sampling rates were set to 256 Hz. Each signal was then divided into 10-second long segments to have higher number of instances for model training. For the GCG dataset, this resulted in 1070 samples for stenosis and 2017 samples for regurgitation; whereas for the SCG dataset, there were 1521 samples for stenosis, and 2017 for regurgitation. No other pre-processing step was applied on the signals.

2.3 Feature Extraction

Considering that the stenosis and regurgitation impairments exhibit different blood flow characteristics, it was hypothesized that there would be differences in the information encoded in the spectral content of the acquired signals. In addition, previous studies showed that VHD assessment can highly benefit from spectral analysis of the SCG signals through spectrogram, wavelet, chromagram and tempogram features (Erin and Semiz, 2023). In this work, a similar approach was inherited, however instead of using a high number of features (and to prevent the possibility of overfitting), only five features (one from the time domain, four from the spectral domain) were extracted from each of the 10-second-long X, Y, Z segments.

- **Entropy:** Entropy quantifies the abrupt energy changes in the time domain of the signal. When the signal exhibits sudden changes, it is expected to observe relatively reduced entropy at the onset of these changes (Hersek et al., 2017).
- **Spectral Entropy:** The interpretation behind spectral entropy is similar to the energy entropy. However computation is carried out in the frequency domain. The resulting value represents how complex the spectrum is, i.e., the larger the complexity, the higher the spectral entropy value (Hersek et al., 2017).
- **Spectral Rolloff:** It measures the frequency at which a specific portion of the signal's energy is concentrated below. Based on the literature, this ratio is usually chosen as 90% (Giannakopoulos and Pikrakis, 2014).
- **Spectral Centroid:** It computes the center of mass of the spectrum. If the signal mostly includes high frequencies, centroid is expected to be relatively higher (Giannakopoulos and Pikrakis, 2014).
- **Spectral Spread:** Spread corresponds to the distribution of the frequencies around the centroid. If the frequencies are tightly gathered around the center frequency, a lower spectral spread value is expected (Giannakopoulos and Pikrakis, 2014).

As there were 5 different features extracted from each of the 10-second-long segments in the X, Y, Z directions, the dataframe was consisting of 15 features, i.e. columns. Segments corresponding to stenosis and regurgitation were labeled as 0 and 1, respectively.

2.4 Model Training and Validation

2.4.1 Stenosis and Regurgitation Classification

Model Selection and Training: In the first task, the aim was to compare the performances of the GCG- and SCG-based stenosis and regurgitation classification models. As the classification model, extreme gradient boosting trees (XGBoost) was chosen. Rather than relying on a single estimator, XGBoost involves employing multiple estimators concurrently. During training, multiple decision trees are trained in an iterative manner, enabling the prediction and refinement of residual errors from the preceding iteration as the training progresses (Dietterich et al., 2002).

For GCG- and SCG-based classification, two different XGBoost models were trained. Before splitting each dataframe into train and test sets, the features were scaled using standard scaler. Following that, the datasets were split into training (80%) and testing (20%) portions. As the dataset had some imbalance regarding the number of samples available in each group, leave-one-out methodology could not be used. During training, the objective function was determined as *binary:logistic*. On the other hand, the default values were used for the remaining parameters. The performance of the model was assessed using accuracy, precision, recall, and f1-score metrics. These equations are presented in Equations 1, 2, 3 and 4, respectively (*TP: true positives, FP: false positives, TN: true negatives and FN: false negatives*). In addition, the area under the receiver operating characteristics curve (ROC AUC) was computed.

$$Accuracy = \frac{TP + TN}{TP + TN + FP + FN} \quad (1)$$

$$Precision = \frac{TP}{TP + FP} \quad (2)$$

$$Recall = \frac{TP}{TP + FN} \quad (3)$$

$$f_1 score = 2 * \frac{precision * recall}{precision + recall} \quad (4)$$

Investigating the Performance of the Individual Axes:

In addition to investigating the performance of SCG and GCG signals in distinguishing between stenosis and regurgitation cases, the performances of the individual GCG and SCG axes (X, Y and Z) were assessed. To that aim, similar feature extraction and model training steps were implemented. Performance assessment was again employed through accuracy, precision, recall, f1-score metrics.

Investigating the Importance of the Spectral Features:

To investigate which features contribute the most in regurgitation and stenosis classification, XG-Boost feature importance ranking was leveraged. In this approach, for each split point, the significance of each attribute in improving the performance measure is computed. The importance scores are then averaged across all decision trees available in the XG-Boost model. The resulting scores are used to rank the features, which represent the importance of the features. Following that, the minimum number of features sufficient was determined to be used in the regression tasks and the redundant features were excluded from the feature set.

2.4.2 Investigating the Cardiovascular Parameter Prediction Performances

After determining the top five most important features in classification of regurgitation and stenosis, those features were used to predict the ejection fraction, left ventricular end diastolic dimension and left ventricular posterior wall thickness values, which were included in the referred database. The reason why only top five features were used was that adding additional features was not increasing the model performances any further. Below, the definition of each cardiovascular parameter and their relationship with the stenosis and regurgitation conditions are detailed.

- *Ejection fraction*: It represents how well the heart pumps blood and is defined as the ratio of the stroke volume and end diastolic left ventricular volume. In case of stenosis and regurgitation, the primary compensatory mechanism required to uphold a normal effective stroke volume is an elevation in left ventricular end-diastolic volume. An increase in end-diastolic volume, results in a decrease in ejection fraction (Maurer, 2006; Chambers, 2006).
- *Left Ventricular Posterior Wall Thickness (LVPW)*: Specifically under aortic stenosis condition, an increase in wall thickness typically occurs to compensate the elevated intracavitary pressure (Chambers, 2006; Mehrotra et al., 2015; Borow et al., 1985).
- *Left Ventricular End Diastolic Dimension (LVEDD)*: Similar to LVPW, an increase is observed in LVEDD in regurgitation (Maurer, 2006), however studies found no significant relationship between LVEDD and stenosis (Mehrotra et al., 2015; Borow et al., 1985).

Using the top five features, separate SCG- and GCG-based XGBoost regression models were trained

Table 1: Performance Metrics for SCG and GCG.

| Signal | Precision | Recall | Accuracy | AUC |
|--------|-----------|--------|----------|------|
| SCG | 94.7 | 94.5 | 94.5 | 0.99 |
| GCG | 96.0 | 95.9 | 95.9 | 0.99 |

Table 2: Performance Metrics for the individual GCG Axes in Classification Task.

| Axis | Precision | Recall | Accuracy | f1-score |
|------|-----------|--------|----------|----------|
| X | 87.5 | 87.5 | 87.5 | 87.5 |
| Y | 87.3 | 87.4 | 87.4 | 87.4 |
| Z | 72.3 | 73.0 | 73.0 | 72.1 |

for each cardiovascular parameter. First, similar to the previous task, the SCG and GCG datasets were split into training (80%) and testing (20%) portions. During training, the objective function was determined as *reg:squarederror* and the remaining parameters were kept as the default values. The performance of the models was assessed using the root mean squared error (RMSE) and mean absolute percentage error (MAPE) metrics. The corresponding equations are presented in Equations 5 and 6, respectively (\hat{y}_i : predicted, y_i : actual).

$$RMSE(y, \hat{y}) = \sqrt{\frac{\sum_{i=0}^{N-1} (y_i - \hat{y}_i)^2}{N}} \quad (5)$$

$$MAPE(y, \hat{y}) = \frac{100\%}{N} \sum_{i=0}^{N-1} \frac{|y_i - \hat{y}_i|}{|y_i|} \quad (6)$$

3 RESULTS AND DISCUSSION

3.1 Stenosis and Regurgitation Classification

Classification Performance: To compare the performance of SCG and GCG in stenosis and regurgitation assessment, two different XGBoost models were trained. The performance results and confusion matrices for both models are presented in Table 1 and Fig. 2. As expected, the GCG-based model resulted in slightly better performance compared to the SCG-based model. Overall, the precision, recall and accuracy values were 94.7, 94.5, and 94.5 for the SCG, and 96.0, 95.9 and 95.9 for the GCG, respectively. On the other hand, both models resulted in an ROC AUC of 0.99.

Assessment of Axes Contributions: Additionally, the performance of the individual GCG and SCG axes in the classification task was investigated. The

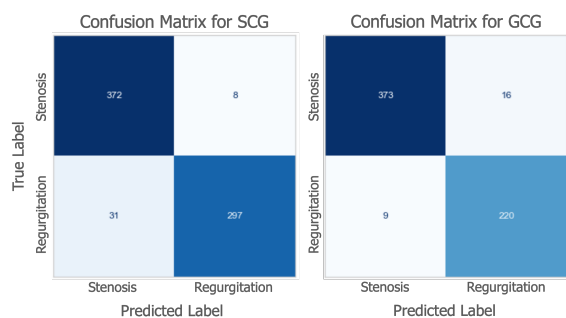


Figure 2: Confusion matrices for the classification models.

Table 3: Performance Metrics for the individual SCG Axes in Classification Task.

| Axis | Precision | Recall | Accuracy | f1-score |
|------|-----------|--------|----------|----------|
| X | 86.9 | 86.9 | 87.2 | 86.8 |
| Y | 86.7 | 86.7 | 86.9 | 86.7 |
| Z | 81.6 | 81.6 | 81.7 | 81.6 |

performance results are presented in Tables 2 and 3 for the GCG- and SCG-based models, respectively. The accuracy values of the models trained with the GCG signals were 87.5 and 87.4 for the X (lateral) and Y (head-to-foot) axes, whereas for the SCG-based models, these values were 87.2 and 86.9, respectively. These findings were indeed in parallel with the previous study (Shandhi et al., 2019). The model trained with the Z (dorso-ventral) axis of the GCG signals resulted in a relatively lower performance compared to the one trained with the SCG signals, with accuracy and f1-score being 73.0 and 72.1, respectively. On the other hand, the one with the SCG signals resulted in an accuracy score of 81.7 and f1 score of 81.6, which is in parallel with the results presented in (Erin and Semiz, 2023). These findings could be attributed to the fact that the flow characteristics of blood can be captured better in the lateral and head-to-foot axes by the GCG as they represent the ejection direction and path; whereas the beating of the heart results in a linear acceleration in the dorso-ventral direction, hence could be better captured by the SCG.

Importance Ranking of Spectral Features: In addition to assessing the performance of the individual axes, importance ranking of the features was also investigated. The top five features for both GCG-based model and SCG-based model are presented in Fig. 3. Indeed, both signal types resulted in the same top five features. The spectral centroid in the lateral and head-to-foot directions appeared as the top two features, showing that the center frequency for blood flow has a distinguishable effect in stenosis and regurgitation

classification. In addition, entropy, which is a time domain feature, did not appear among the top features. Another important observation was that features from the dorso-ventral axis have relatively lower importance compared to the features from the lateral and head-to-foot directions.

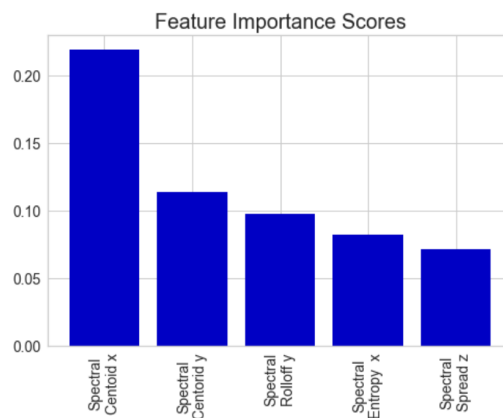


Figure 3: Feature importance scores for the SCG and GCG models.

Table 4: Performance Metrics for SCG Regression Task.

| SCG | Ejection Fraction | LVEDD | LVPW |
|------|-------------------|-------|------|
| RMSE | 11.5 | 10.6 | 1.71 |
| MAPE | 19.4 | 15.5 | 12.0 |

Table 5: Performance Metrics for GCG Regression Task.

| GCG | Ejection Fraction | LVEDD | LVPW |
|------|-------------------|-------|------|
| RMSE | 11.9 | 10.0 | 1.85 |
| MAPE | 20.6 | 14.5 | 13.1 |

3.2 Cardiovascular Parameter Prediction Results

Using the top five features, separate SCG- and GCG-based XGBoost regression models were trained for each of ejection fraction (EF), left ventricular posterior wall thickness (LVPW) and left ventricular end diastolic dimension (LVEDD). The RMSE and MAPE values for the SCG- and GCG-based models are presented in Table 4 and 5, respectively. The results show that the SCG and GCG have comparable performance in the estimation of all three parameters. While the (RMSE, MAPE) values were (11.5, 19.4), (10.6, 15.5), (1.71, 12.0) for the SCG-based models, these values were (11.9, 20.6), (10.0, 14.5), (1.85, 13.1) for the GCG-based models for ejection fraction, LVEDD and LVPW, respectively. SCG-based models performed slightly better than the GCG ones in the estimation of ejection fraction and LVPW, whereas LVEDD estimation resulted in relatively lower error

when GCG was used. Overall, it can be deduced that both SCG and GCG can potentially be leveraged in the estimation of cardiovascular parameters.

4 CONCLUSION

In this work, the performances of the SCG- and GCG-based models in stenosis and regurgitation assessment were investigated. Additionally, the predictive performances of SCG- and GCG-based models on the cardiovascular parameters (ejection fraction, left ventricular end diastolic dimension and left ventricle posterior wall thickness) under stenosis and regurgitation conditions were studied. Overall, it was found that the GCG-based model performs slight better than the SCG-based model in distinguishing between the stenosis and regurgitation cases, most probably as the GCG could capture the angular characteristics of the blood flow better than the SCG. Additionally, the best performing axes were found to be the lateral and head-to-foot axes.

For the regression tasks, the SCG and GCG had comparable performance in the estimation of ejection fraction, left ventricular posterior wall thickness and left ventricular end diastolic dimension. Models based on SCG demonstrated slightly higher performance compared to those based on GCG in estimating ejection fraction and LVPW. On the other hand, the estimation of LVEDD showed a relatively lower error when GCG-based model was used. In conclusion, it can be inferred that both SCG and GCG can potentially be used in estimating various cardiovascular parameters.

Future work will focus on improving the current pipelines further to enable real-time monitoring of VHDs and validating these pipelines in larger datasets to ensure generalizability.

REFERENCES

- Borow, K. M., Colan, S., and Neumann, A. (1985). Altered left ventricular mechanics in patients with valvular aortic stenosis and coarction of the aorta: effects on systolic performance and late outcome. *Circulation*, 72(3):515–522.
- Chambers, J. (2006). The left ventricle in aortic stenosis: evidence for the use of ace inhibitors. *Heart*, 92(3):420–423.
- Dietterich, T. G. et al. (2002). Ensemble learning. *The handbook of brain theory and neural networks*, 2(1):110–125.
- Erin, E. and Semiz, B. (2023). Spectral analysis of cardiac vibrations to distinguish between valvular heart diseases.
- Faisal, I. A., Purboyo, T. W., and Ansori, A. S. R. (2019). A review of accelerometer sensor and gyroscope sensor in imu sensors on motion capture. *J. Eng. Appl. Sci.*, 15(3):826–829.
- Giannakopoulos, T. and Pikrakis, A. (2014). *Introduction to audio analysis: a MATLAB® approach*. Academic Press.
- Go, A. S., Mozaffarian, D., Roger, V. L., Benjamin, E. J., Berry, J. D., Borden, W. B., Bravata, D. M., Dai, S., Ford, E. S., Fox, C. S., et al. (2013). Heart disease and stroke statistics—2013 update: a report from the american heart association. *Circulation*, 127(1):e6–e245.
- Hersek, S., Pouyan, M. B., Teague, C. N., Sawka, M. N., Millard-Stafford, M. L., Kogler, G. F., Wolkoff, P., and Inan, O. T. (2017). Acoustical emission analysis by unsupervised graph mining: A novel biomarker of knee health status. *IEEE Transactions on Biomedical Engineering*, 65(6):1291–1300.
- Inan, O. T., Migeotte, P.-F., Park, K.-S., Etemadi, M., Tavakolian, K., Casanella, R., Zanetti, J., Tank, J., Funtova, I., Prisk, G. K., et al. (2014). Ballistocardiography and seismocardiography: A review of recent advances. *IEEE journal of biomedical and health informatics*, 19(4):1414–1427.
- Jafari Tadi, M., Lehtonen, E., Saraste, A., Tuominen, J., Koskinen, J., Teräs, M., Airaksinen, J., Pänkäälä, M., and Koivisto, T. (2017). Gyrocardiography: A new non-invasive monitoring method for the assessment of cardiac mechanics and the estimation of hemodynamic variables. *Scientific reports*, 7(1):1–11.
- Klabunde, R. (2011). *Cardiovascular physiology concepts*. Lippincott Williams & Wilkins.
- Maurer, G. (2006). Aortic regurgitation. *Heart*, 92(7):994–1000.
- Mehrotra, P., Flynn, A. W., Jansen, K., Tan, T. C., Mak, G., Julien, H. M., Zeng, X., Picard, M. H., Passeri, J. J., and Hung, J. (2015). Differential left ventricular outflow tract remodeling and dynamics in aortic stenosis. *Journal of the American Society of Echocardiography*, 28(11):1259–1266.
- Shandhi, M. M. H., Semiz, B., Hersek, S., Goller, N., Ayazi, F., and Inan, O. T. (2019). Performance analysis of gyroscope and accelerometer sensors for seismocardiography-based wearable pre-ejection period estimation. *IEEE journal of biomedical and health informatics*, 23(6):2365–2374.
- Svensson, L. (2008). Aortic valve stenosis and regurgitation: an overview of management. *Journal of Cardiovascular Surgery*, 49(2):297.
- WHO (2020). The top 10 causes of death. *Geneva: World Health Organization*. <https://www.who.int/news-room/fact-sheets/detail/the-top-10-causes-of-death> (visited: 2022-09).
- Yang, C., Fan, F., Aranoff, N., Green, P., Li, Y., Liu, C., and Tavassolian, N. (2021). An open-access database for the evaluation of cardio-mechanical signals from pa-

tients with valvular heart diseases. *Frontiers in Physiology*, 12.

Yang, C., Tang, S., and Tavassolian, N. (2017). Utilizing gyroscopes towards the automatic annotation of seismocardiograms. *IEEE Sensors Journal*, 17(7):2129–2136.

Yang, C. and Tavassolian, N. (2017). Combined seismo-and gyro-cardiography: A more comprehensive evaluation of heart-induced chest vibrations. *IEEE journal of biomedical and health informatics*, 22(5):1466–1475.

